PHASE-LIFETIME SPECTROSCOPY OF PHOTOCYCLE PROCESSES

Proton Release and Uptake Kinetics of Purple Membrane

MARK H. SINTON AND T. G. DEWEY
Department of Chemistry, University of Denver, Denver, Colorado 80208

ABSTRACT Phase-lifetime spectroscopy was used to measure the kinetics of light-driven proton transients and M intermediate decay of purple membrane. The kinetics were measured in distilled water and in 0.4 M KCl over the pH range of 5.3–8.8. The low ionic strength data showed results that were comparable to previous data. The lifetimes for the decay of the proton transient were intermediate between the two M decay lifetimes. Deviations from this behavior occurred at pH 5.3. The high-salt data showed two proton transients: a release process with a lifetime similar to the fast M decay, and an uptake process with a lifetime similar to the slow M decay. The release process is not seen in flash experiments. This difference is due to differences in the amplitudes of the relaxation processes for the two types of experiments. The high-salt data showed little pH dependence below pH 7.8. Both sets of data were shown to be consistent with a single mechanism that correlates the M kinetics with the proton kinetics. The proposed mechanism consists of the parallel formation and decay of two M intermediates that can interconvert. Only one of the intermediates results in a proton being released from the bacteriorhodopsin. Thus, this mechanism has a nonproductive pathway as well as a productive pathway in which a single proton is pumped. Detailed kinetic expressions are derived for this mechanism for the phase-lifetime and flash kinetic experiment. These results could explain the qualitative features of the distilled water data and provide a quantitative description of the high-salt data. Expressions for the quantum yield and the H^+ to M ratio were derived in terms of the individual rate constants of the mechanism. Conditions are established in which the quantum yield for proton release can vary with only small changes in the M/H^+. This reconciles an apparent conflict in previous evidence from flash experiments and demonstrates the difficulty of determining stoichiometry from kinetic amplitude information.

INTRODUCTION

Bacteriorhodopsin (bR), the light-driven proton pump from *Halobacterium halobium,* has received considerable attention because it is a relatively simple system for investigating primary events in photosynthesis and ion transport. Although there have been numerous studies of the bR photocycle (for a review see reference 1), a kinetic mechanism describing the photocycle has yet to be agreed upon (cf. 2, 3). The number of studies on the kinetics of light-driven proton transport has been much more restrictive. Most work has concentrated on measuring proton transients, resulting from illuminating purple membrane in unbuffered solutions (4–6). One difficulty in such work is that the bR photocycle covers such a broad spectral range that interference of this signal with a pH indicator cannot be avoided. Consequently, the photocycle signal must be subtracted from the combined signal. While this makes the experiment more complicated, with the necessary precautions a proper subtraction can be achieved. Recent work by Grzesiek and Dencher used flash spectroscopy to determine the time course and stoichiometry of the proton release kinetics (5). Determining stoichiometry from an analysis of decay amplitudes, they found one proton released per photocycling molecule. This stoichiometry increased only slightly (28%) from low to high ionic strength. These results are in agreement with previous kinetic data from other groups (6, 7). However, they are in apparent disagreement with the results of Ort and Parsons who used a photocalorimetry technique to demonstrate that the quantum yield of proton release increased by ~75% when going from low to high ionic strength (8). Ort and Parsons also measured M intermediate amplitudes at a time that was 2 ms after the actinic flash. These amplitudes were used to determine the stoichiometry of proton release per photocycle. Their results are consistent with a stoichiometry of proton release of 1 per photocycle at low salt and 2 per photocycle at high salt.

In the present work, the light-driven kinetics of proton release and uptake by purple membrane was investigated using phase-lifetime spectroscopy. The M state kinetics were measured in parallel experiments. In both cases, the

Correspondence should be addressed to Dr. Dewey.

kinetics were determined at high and low ionic strength and as a function of pH. A previous paper in this series described how amplitude dispersion curves obtained with this technique can be analyzed to determine kinetic parameters of photocycle processes (9). In general, phase-lifetime spectroscopy gives the same information as flash techniques. However, sometimes the amplitudes of a given process will change between the two techniques. This is a result of contributions to the rate process from steady-state concentrations of intermediates, which occur in the phase-lifetime experiment. Thus, there can be instances in which the two techniques will have a different weighting of the relative amplitudes in multiple relaxation processes. The differences in flash and phase amplitudes are demonstrated in this work by deriving amplitude expressions for each technique for a specific mechanism. Our experimental results show a distinct difference between the high- and low-salt proton release kinetics over most of the pH range. These proton kinetic results are quantitatively interpreted in terms of a specific reaction mechanism. The proposed mechanism is also consistent with the M intermediate kinetics. This mechanism has two M states that can interconvert. Only one of these states can undergo productive proton transport. This model can account for the variability of the quantum yield for proton release within the framework of a model in which only one proton is transported. A theoretical analysis of the amplitudes of this model is presented for both the phase and the flash experiments. It is shown that using kinetic amplitudes to determine stoichiometry can give erroneous results. This is true even when the decay time is well separated from the rise time of the process of interest. The theoretical analysis allows an estimate of the ionic strength dependence of the quantum yield of proton transport and of the M_{412}/H^+ amplitude ratio. This analysis shows that the quantum yield results of Ort and Parsons (8) are not necessarily inconsistent with the M_{412}/H^+ amplitude ratios determined by Grzesiek and Dencher (5).

MATERIALS AND METHODS

Chemicals

2',7'-Dichlorofluorescein (pK_a 5.9) and *p*-nitrophenol (pK_a 6.8) were obtained from Eastman Organic Chemicals (Rochester, NY) and were recrystallized from a 50:50 (vol/vol) ethanol-water mixture. 7-Hydroxycoumarin (pK_a 7.8) was obtained from Sigma Chemical Co. (St. Louis, MO) and used without further purification. *m*-Nitrophenol (pK_a 8.6) was from Aldrich Chemical Co. (Milwaukee, WI) and was used without further purification. All other chemicals were reagent grade.

Purple Membrane and Sample Preparation

Halobacteria halobium S-9 was cultured on defined media (10). Purple membrane fragments were purified by sucrose step gradient (11). All kinetic measurements were done on samples with an optical density of 0.7 at 568 nm. Samples were either in distilled water (referred to as the low-salt system) or in 0.4 M KCl (high-salt system). All absorbances were measured on a Cary 219 UV-Vis spectrometer (Varian, Chicago, IL). The pH values of the samples were measured with a model 611 pH meter (Orion Research Inc., Cambridge, MA) and adjusted with small volumes of acid or base. The concentration of the pH indicator in the various samples was as follows: pH 5.3 and 5.8 had 48 and 10 μM of 2',7'-dichlorofluorescein, respectively; pH 6.3 and 6.8 had 150 and 75 μM of *p*-nitrophenol, respectively; pH 7.3 and 7.8 had 38 μM of 7-hydroxycoumarin; and pH 8.3 and 8.8 had 300 μM of *m*-nitrophenol. Indicator concentrations were varied to obtain similar absorbances at the different pH conditions. The pH was monitored by the absorbance at the following peaks: 500 nm for 2',7'-dichlorofluorescein; 400 nm for *p*-nitrophenol; 320 nm for 7-hydroxycoumarin; and 380 nm for *m*-nitrophenol. All dyes were dissolved in distilled water to make stock solutions with the exception of 2',7'-dichlorofluorescein, which was dissolved in dimethylsulfoxide (DMSO). DMSO never exceeded 3% of the sample.

Kinetic Measurements

Proton uptake and release kinetics of bacteriorhodopsin were measured using the phase-lifetime spectrophotometer described previously (12, 13). The actinic light source was changed to a 150-W miniature Xenon arc lamp model 66030 (Oriel Corp., Stratford, CT), which was powered by an Oriel 200-W power supply. This lamp was filtered with an Oriel infrared heat filter and a 560 ± 10 nm interference filter. A 15-cm focal length lens focused the actinic light onto the sample.

Because the spectral response of the photocycle overlaps with the spectral changes of the pH indicator, it was necessary to correct the measured signals to eliminate the contribution of the bacteriorhodopsin photocycle. The signal response was measured in the absence and presence of indicator dye. Before adding dye, the phase of the detector was adjusted to give a quadrature reading of zero, and the "in-phase" signal amplitude and phase setting were recorded. This procedure was followed for each chopping frequency selected. The frequencies were recorded from 31 to 8,710 rad/s. After addition of dye, the photomultiplier DC voltage decreased due to the increased absorbance of the sample, resulting in a lower background light intensity. The modulated actinic light was then applied to the sample, and the phase was set to the value recorded for the sample without dye at the corresponding frequency. The quadrature and "in-phase" signal amplitudes were then measured. The amplitude of the signal is the sum of the "in-phase" amplitude plus the quadrature amplitude. However, these signals represent transmittance and not absorbance signals so that a direct subtraction of the signal with and without indicator is not valid. To convert to absorbance units, the modulated amplitudes are divided by the appropriate DC level on the phototube. This quantity is an accurate measure of absorbance because the modulated signal is only 0.1% of the DC signal. Thus, the amplitude properly corrected for interference from the photocycle is given by

$$A = (I/I')(A_{0^\circ,\mathrm{dye}} + A_{90^\circ,\mathrm{dye}}) - A_{0^\circ}, \qquad (1)$$

where $A_{0^\circ,\mathrm{dye}}$ and $A_{90^\circ,\mathrm{dye}}$ is the "in-phase" and quadrature amplitude of the sample containing dye, A_{0° is the amplitude of the sample without dye, I is the DC level on the phototube before dye is added, and I' is the DC level after

dye was added. An alternate approach to this subtraction might be to adjust the photomultiplier high voltage so I and I' are identical. This procedure does not result in an appropriate subtraction of the photocycle signal because the gain of the photomultiplier is dependent on its high voltage. Amplitude dispersion curves were obtained from the frequency dependence of the calculated amplitude, A. At low actinic light intensities, the amplitude response for the "on" and "off" cycles will be alternately exponential rise and decays with the same time constant (9). With this situation at any phase setting of the lock-in amplifier, the amplitudes, $A_{0°}$ and $A_{90°}$, will always add to give the overall signal amplitude. This was established experimentally when observing the M intermediate signal over a range of chopping frequencies. The amplitude dispersion curves for both the photocycle signal and the indicator signal were analyzed using the expression derived previously (Eq. 13, reference 9).

$$A = \sum_{i=1}^{k} \sum_{n=0} \frac{[A]_i \sin [(2n + 1)(\pi/2 + \phi_{0,i}) - \phi_{n,i}]}{(2n + 1)^2 [1 + \omega^2 \tau_i^2 (2n + 1)^2]^{1/2}}, \quad (2)$$

where the summation over i represents the sum of the reaction modes, and the summation over n represents the harmonics of each response function. The second summation can be adequately represented by truncating the series at $n = 50$. The value of k depends upon the specific data set. For the M intermediate, k must equal 2 in order to adequately fit the data. The quantities, $[A]_i$ and τ_i, represent the amplitude and lifetime of the ith mode of the reaction, respectively. The phase shift for each harmonic is given by $\tan \phi_{n,i} = (n + 1)\, \omega\tau_i$. Eq. 2 takes into account the harmonic sensitivity of the specific "lock-in" amplifier used in this study. Experimental data were fit to Eq. 2 using a nonlinear least squares routine. The fitted parameters were the amplitudes and lifetimes. The M intermediate was measured at 400 nm, and the dye signals were measured at their absorbance maxima. The M signal showed comparable decay kinetics at 365 nm, indicating no contribution from other photostates at these wavelengths.

RESULTS

Representative amplitude dispersion curves for the pH indicator response are shown in Figs. 1–4. These curves show the experimental amplitudes, as determined by Eq. 1, as a function of frequency. The solid lines are the nonlinear least squares fit obtained using Eq. 2. Fig. 1 shows the amplitude dispersion curve for purple membrane in distilled water at pH 6.8. This curve could be fit with a single relaxation process. The comparable curve at 0.4 M KCl

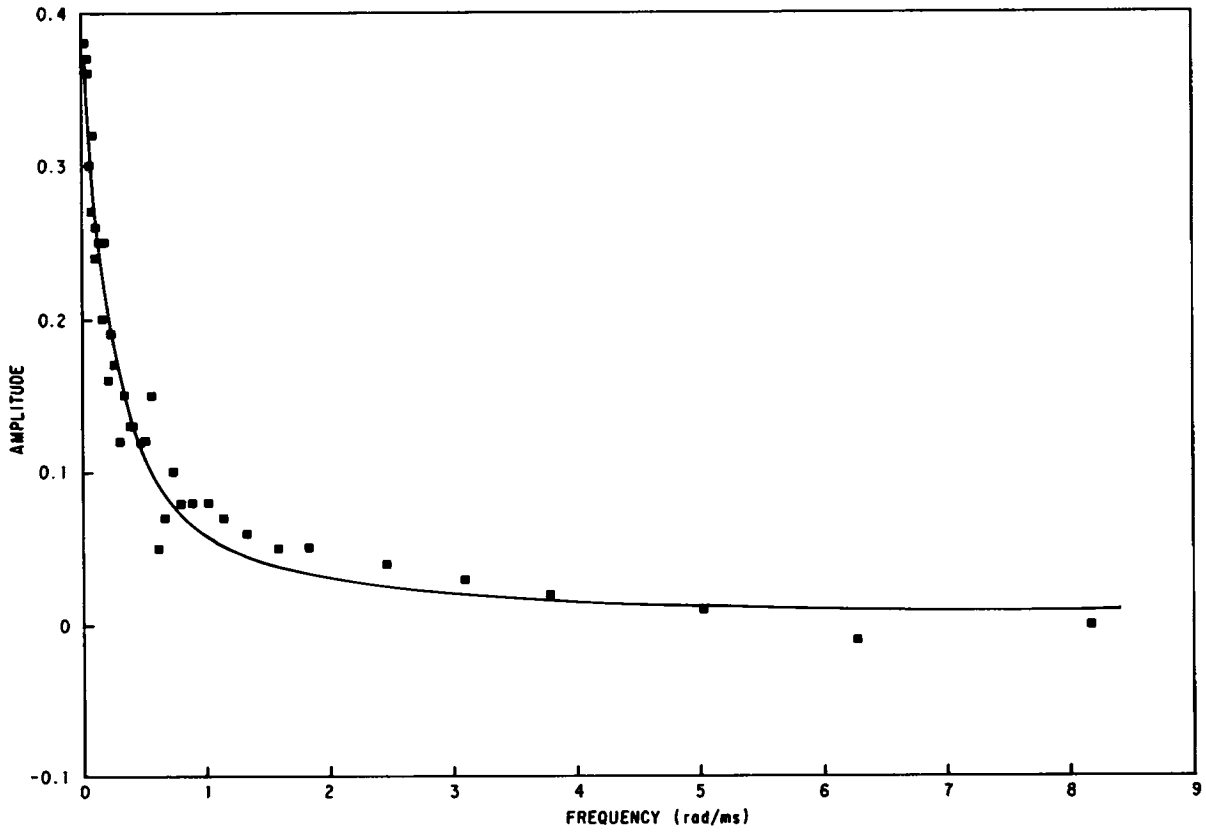

FIGURE 1 Plot of pH indicator absorbance amplitudes versus chopper frequency. Sample contained 1.8×10^{-5} M bacteriorhodopsin in distilled water at pH 6.8. The pH indicator dye used was p-nitrophenol at a final concentration in the sample of 75 μM. Experimental amplitudes were determined using Eq. 1. Solid line shows nonlinear least squares fit using Eq. 2. One relaxation process was observed corresponding to proton uptake.

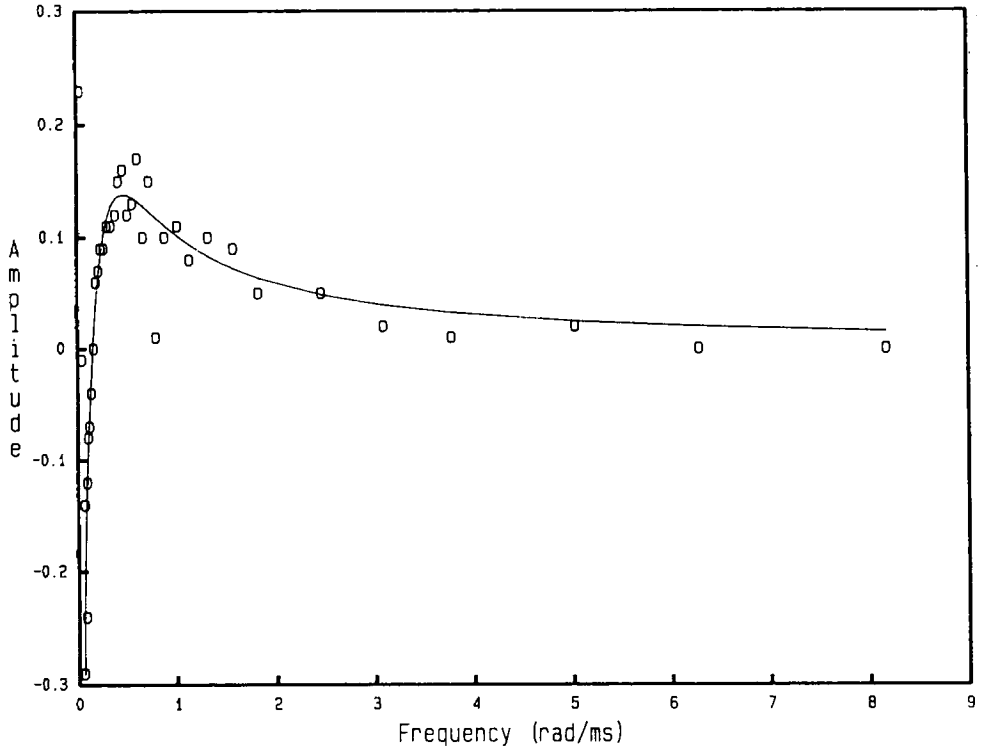

FIGURE 2 Plot of pH indicator absorbance amplitudes versus chopper frequency. Sample contained 1.8×10^{-5} M bacteriorhodopsin and 75 μM of the pH indicator dye p-nitrophenol in 0.4 M KCl at pH 6.8. Experimental amplitudes were determined using Eq. 1. Solid line shows nonlinear least squares fit using Eq. 2. Two relaxation processes of opposite sign were observed, corresponding to proton uptake and release.

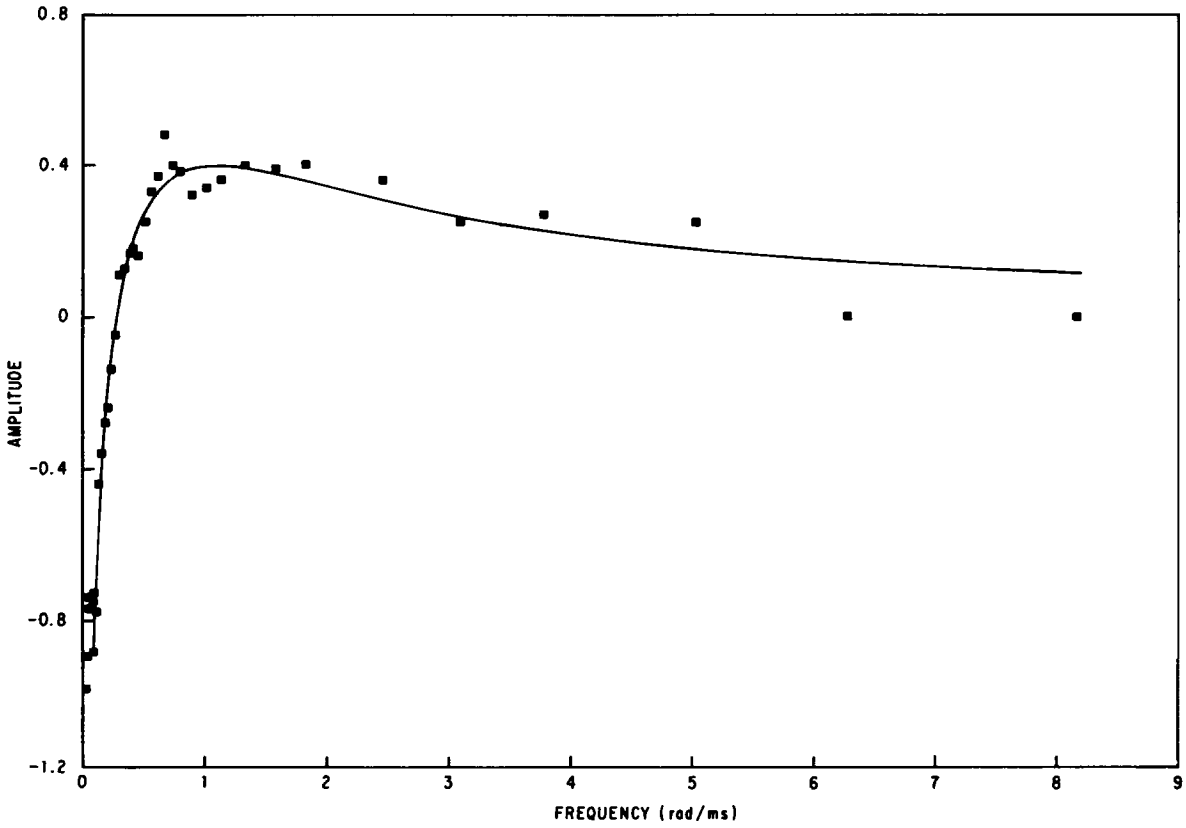

FIGURE 3 Plot of pH indicator absorbance amplitudes versus chopper frequency. Sample contained 1.8×10^{-5} M bacteriorhodopsin and 48 μM of the pH indicator dye 2', 7'-dichlorofluorescein in distilled water at pH 5.3. Experimental amplitudes were determined using Eq. 1. Solid line shows nonlinear least squares fit using Eq. 2. Note that two relaxation processes of opposite sign were observed, similar to high-salt behavior.

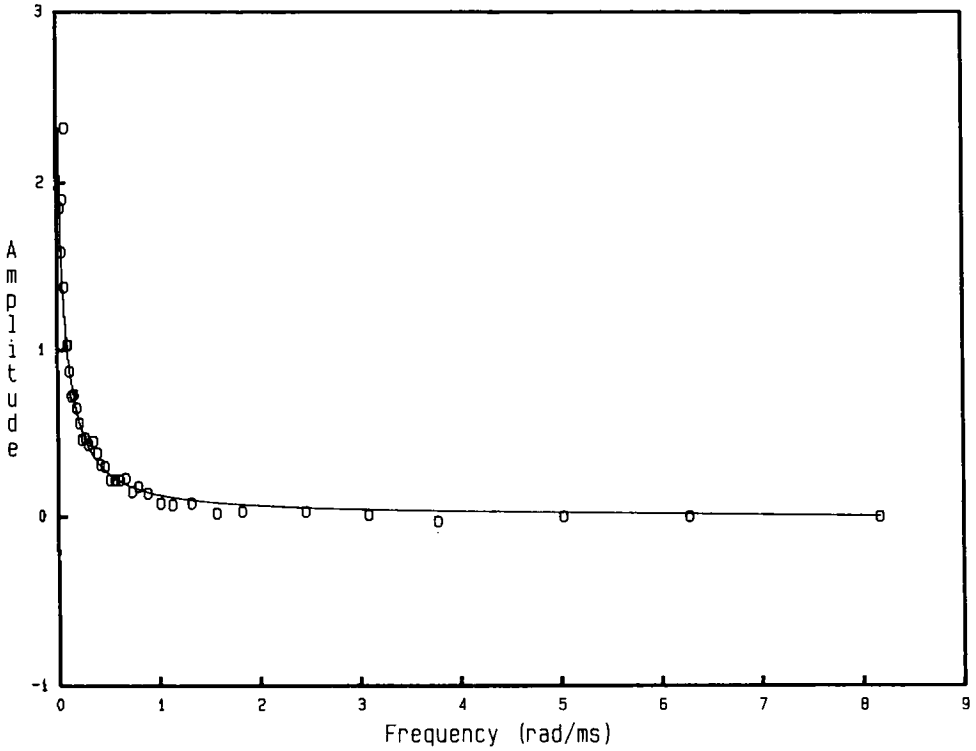

FIGURE 4 Plot of pH indicator absorbance amplitudes versus chopper frequency. Sample contained 1.8×10^{-5} M bacteriorhodopsin and 300 μM *m*-nitrophenol in 0.4 M KCl at pH 8.8. Experimental amplitudes were determined using Eq. 1. Solid line shows nonlinear least squares fit using Eq. 2. Note that only one relaxation process was observed, similar to low-salt behavior.

(pH 6.8) is shown in Fig. 2. It contains contributions from two relaxation processes with amplitudes of opposite signs. This suggests that purple membrane at high salt has a proton release and a proton uptake relaxation process on a comparable time scale. Fig. 3 shows the amplitude dispersion curve at pH 5.3 for purple membrane in distilled water. At this low pH, the curves begin to resemble the high-salt curves and require a four parameter fit (two amplitudes and two lifetimes). Fig. 4 shows data for 0.4 M KCl at pH 8.8. At this high pH, the high-salt curves begin to resemble those for distilled water and could be fit with a single relaxation process. For all sets of conditions, the amplitude dispersion curves for the M intermediates were also determined (data not shown). In all cases, two relaxation processes of identical sign were required to fit the M kinetics. These relaxation processes represent the M decay kinetics. Under the conditions of this phase-lifetime experiment, the M formation kinetics are not resolved (cf. 9). The experimentally determined M decay lifetimes and amplitudes and the lifetime of proton uptake for all of the experiments in distilled water are shown in Table I. These

TABLE I
PROTON UPTAKE AND M_{412} DECAY KINETICS pH DEPENDENCE IN DISTILLED WATER*

pH	Proton uptake	M_{412} Decay		
	H	τ_1	τ_2	A_1/A_2
	ms	*ms*	*ms*	
5.3	0.66 (18)	4.7	21	0.47
5.8	8.8	4.0	21	0.81
6.3	3.2	3.5	16	0.34
6.8	4.4	2.4	15	0.38
7.3	9.4	3.0	10	0.52
7.8	8.0	1.9	12	0.16
8.3	15	2.9	19	0.16
8.8	14	3.5	12	0.55

*At pH 5.3, the low-salt system behaves like a high-salt system and requires two relaxation processes of opposite sign to fit the data. τ_2 is shown in parentheses. Amplitude ratio of fast relaxation amplitude, A_1, to slow relaxation amplitude, A_2. Relaxation times have error limits of 10% and amplitudes are 20% as determined by the nonlinear least squares fitting routine.

TABLE II
PROTON RELEASE AND UPTAKE KINETICS AND M_{412} DECAY KINETICS pH DEPENDENCE IN 0.4 M KCl*

pH	Proton kinetics		$R^{obs}(R_1^{calc})(R_2^{calc})$	M_{412} decay		
	τ_1	τ_2		τ_1	τ_2	A_1/A_2
	ms	*ms*		*ms*	*ms*	
5.3	2.2	20	−2.0(−1.9)(−0.2)	3.7	17	1.1
5.8	3.1	18	−1.7(−1.1)(−1.6)	2.9	17	2.2
6.3	2.7	5.5	−0.97(−2.1)(−0.5)	2.8	10	1.2
6.8	3.0	7.5	−1.5(−1.6)(−1.8)	1.6	7.4	0.8
7.3	4.1	7.0	−2.3(−1.2)(−0.8)	2.7	21	2.3
7.8	1.2	22	−11(−4.0)(−1.9)	1.9	70	0.1
8.3	9.0			2.1	32	0.2
8.8	14			1.5	53	0.1

*τ_1 corresponds to a proton release process, and τ_2 corresponds to proton uptake. R is the ratio of the relaxation amplitudes for the proton release processes. A_1/A_2 is the ratio of the relaxation amplitudes for the M_{412} decay processes. R_1 calculated assuming a λ_2 of 357 s^{-1}. R_2 calculated assuming a λ_2 of 255 s^{-1}. Note that at pH 8.3 and 8.8, the high-salt data behaves like a low-salt system. Only one relaxation process is required to fit the data.

results are consistent with previous data (5) and show the proton uptake lifetime being intermediate between the two lifetimes for the decay of the M intermediates. These results show small pH effects in this region as previously noted (14). Table II lists the amplitude ratios and lifetimes for the pH indicator response at 0.4 M KCl as a function of pH. The M lifetimes and amplitudes are also shown. Again there is little pH dependence. These results show a proton uptake process with a lifetime approximately identical to the slow decay of the M intermediate. A proton release process is seen with a lifetime equal to approximately that of the fast M decay. This process is much slower than the M formation processes observed in flash experiments. These results differ from previous flash results (5). At high salt, the flash experiments show a single proton uptake process with a relaxation time identical to that of the slow decay of the M intermediate. As will be discussed later, the reason for observing the second process in the phase and not in the flash experiment is due to the difference in the techniques. The amplitude of the second process contributes much more strongly in a phase-lifetime experiment. The basis for this effect is seen clearly by deriving expressions for the amplitudes for each experiment. This is done in the next section for a specific reaction mechanism.

Analysis of Kinetic Data

The kinetic results were used to test a variety of photocycle mechanisms. The main features of these results, which were used in discriminating mechanisms, were: (*a*) The mechanism must show a single proton uptake process (low-salt results) with a lifetime in-between those for the two *M* intermediate lifetimes. (*b*) With a suitable adjustment of parameters due to salt effects, the identical mechanism must show a proton release and proton uptake process with lifetimes comparable to the fast and slow *M* decay processes, respectively. This will account for the high-salt data. (*c*) The experimental amplitude ratios of the proton release and proton uptake processes at high salt must be quantitatively predicted using the lifetime data and reasonable estimates for any adjustible parameters.

Using these criteria for testing a variety of mechanisms, the following mechanism was found to be the most consistent with the experimental results:

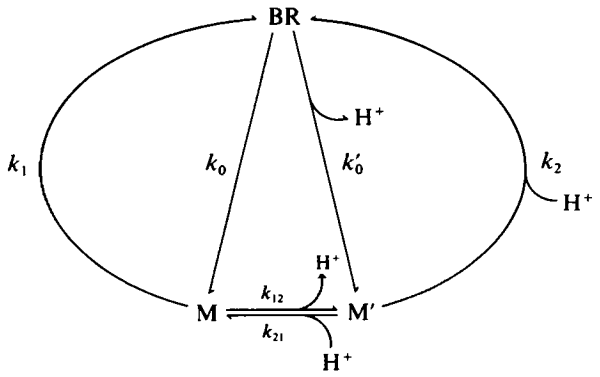

The rate expressions for this mechanism have been derived along with expressions for the observable parameters in the phase-lifetime and flash experiments. For the phase-lifetime experiments, one must solve the rate equations for both the "on" and "off" cycles (9). The rate laws for the "on" cycle is given by

$$\mathrm{d}[\mathrm{M}]/\mathrm{d}t = k_0[\mathrm{BR}] + k_{21}[\mathrm{M}'] - (k_{12} + k_1)[\mathrm{M}]$$
$$\mathrm{d}[\mathrm{M}']/\mathrm{d}t = k_0'[\mathrm{BR}] + k_{12}[\mathrm{M}] - (k_{21} + k_2)[\mathrm{M}'], \quad (3)$$

where the rate constants are defined by the above diagram, and the constants k_0 and k_0' are considered to be linearly dependent on light intensity (cf. 9). In addition to the rate expressions in Eq. 3, the conservation relation is also used. It is $[\mathrm{BR}]_{tot} = [\mathrm{BR}] + [\mathrm{M}] + [\mathrm{M}']$, where $[\mathrm{BR}]_{tot}$ is the total bacteriorhodopsin concentration. Eq. 3 may be readily solved by performing a Laplace transform on the rate expressions, solving the resulting algebraic equations, and then performing the inverse transform on the solution to the algebraic equations. To solve the equations for the "off" cycle, all that is required is to set $k_0 = k_0' = 0$. When this is done, expressions of the following form are obtained:

$$A(t) = \Sigma\,[A_i - (A_i - B_i)e^{-t/\tau_i}] \quad \text{"on" cycle}$$
$$A(t) = \Sigma\, B_i\, e^{-t/\tau_i} \quad \text{"off" cycle,} \quad (4)$$

where A is a concentration variable and the summation runs over the relaxation modes, τ_i is the relaxation time of the ith mode, and A_i and B_i are amplitudes for the ith modes. It was previously shown (9) that the amplitude response function in a phase-lifetime experiment is given by

$$A(\omega) = \Sigma\, 2\, A_i \tanh(\pi/2\,\omega\tau_i). \quad (5)$$

Eq. 2 represents a weighting of this function to account for the harmonic sensitivity of the specific lock-in amplifier used in this work. The resulting amplitude response functions for the M and M' photocycle states are quite complicated. It contains terms in which the steady-state concentration of all the variables appears. Since relatively low actinic light intensities are used in the phase-lifetime experiments, approximately only 1% of the bacteriorhodopsin is in the M state. This means that only the terms involving [BR] will have a significant contribution to the response functions. Because the expressions for the M states contain a mixing of the normal modes of the reaction, contributions of the [BR] terms appear in the expressions for the steady-state levels of these states. These terms are given by Eq. 6:

$$[\mathrm{M}] = \sum_{i=1}^{3} 2A_i \tanh(\pi/2\,\omega\tau_i)$$
$$[\mathrm{M}'] = \sum_{i=1}^{3} 2A_i' \tanh(\pi/2\,\omega\tau_i'), \quad (6)$$

where

$$A_1 = \frac{k_0[\mathrm{BR}]k_{21}}{1/\tau_1(1/\tau_1 - 1/\tau_2)} - \frac{k_0[\mathrm{BR}]k_{21}k_{12}}{1/\tau_1(1/\tau_1 - 1/\tau_2)(\lambda_1 - 1/\tau_1)}$$

$$A_2 = \frac{-k_0[\mathrm{BR}]k_{21}}{1/\tau_2(1/\tau_1 - 1/\tau_2)} + \frac{k_0[\mathrm{BR}]k_{21}k_{12}}{1/\tau_2(1/\tau_1 - 1/\tau_2)(\lambda_1 - 1/\tau_2)}$$

$$A_3 = \frac{-k_0[\mathrm{BR}]}{\lambda_1} + \frac{k_0[\mathrm{BR}]k_{21}k_{12}}{\lambda_1(1/\tau_1 - \lambda_1)(1/\tau_2 - \lambda_1)}$$

$$A'_1 = \frac{k'_0[\mathrm{BR}]k_{12}}{1/\tau_1(1/\tau_1 - 1/\tau_2)} - \frac{k'_0[\mathrm{BR}]k_{21}k_{12}}{1/\tau_1(1/\tau_1 - 1/\tau_2)(\lambda_2 - 1/\tau_1)}$$

$$A'_2 = \frac{-k'_0[\mathrm{BR}]k_{12}}{1/\tau_2(1/\tau_1 - 1/\tau_2)} + \frac{k'_0[\mathrm{BR}]k_{21}k_{12}}{1/\tau_2(1/\tau_1 - 1/\tau_2)(\lambda_2 - 1/\tau_2)}$$

$$A'_3 = \frac{-k'_0[\mathrm{BR}]}{\lambda_2} + \frac{k'_0[\mathrm{BR}]k_{21}k_{12}}{\lambda_2(1/\tau_1 - \lambda_2)(1/\tau_2 - \lambda_2)}$$

$$1/\tau_3 = \lambda_1 = k_{12} + k_1; \qquad 1/\tau'_3 = \lambda_2 = k_{21} + k_2$$

$$1/\tau_{1,2} = 1/\tau'_{1,2} = \frac{(\lambda_1 + \lambda_2) \pm \sqrt{(\lambda_1 - \lambda_2)^2 + 4k_{12}k_{21}}}{2}.$$

The fast relaxation time in the last equation (+ root) is defined as τ_1 and the slow relaxation time (− root) is τ_2. These expressions can be slightly simplified using the following, useful relationships:

$$1/\tau_1 + 1/\tau_2 = \lambda_1 + \lambda_2$$
$$(1/\tau_1)(1/\tau_2) = \lambda_1\lambda_2 - k_{21}k_{12}. \qquad (7)$$

These theoretical results can be used to interpret the experimental data. In the above model, the M′ state represents a deprotonated protein state, so the observed [H^+] transients should be directly proportional to the M′ concentration. The M state represents a state in which the retinal's Schiff base linkage has been deprotonated but no proton appears in the medium. The photocycle kinetics observed by absorbance at 412 nm is the summed contributions of the M and M′ responses. The low salt proton data are predicted when the product $k_{12}k_{21}$ makes a significant contribution in the expressions for $1/\tau_1$ and $1/\tau_2$. This results in $1/\tau'_3$ being intermediate between the values for $1/\tau_1$ and $1/\tau_2$. Additionally, these conditions result in A'_3 being greater than A'_2 or A'_1. The observed proton uptake time is intermediate between the two M decay times. However, this time may not be exactly equal to τ'_3 as A'_1 and A'_2 may make some contribution to the signal. This contribution is not large enough to allow the resolution of separate processes but is large enough to make an accurate determination of $1/\tau'_3$ difficult. To get a feeling for the relative contributions of each mode, it is instructive to do a rough estimate. Using the average relaxation time over the entire pH range for proton uptake, and for the two M decays (Table I), λ_2, $1/\tau_1$, and $1/\tau_2$ are estimated to be 104, 330, and 67 s^{-1}, respectively. This allows a calculation of a value of 293 s^{-1} for λ_1. From this last value, it would not be unreasonable for k_{12} to be of the order of 100 s^{-1}. Using Eqs. 6 and 7, the relative contribution of A'_1, A'_2, and A'_3 to the proton relaxation are 5, 26, and 69%.

For this mechanism to be consistent with the low-salt photocycle results, the contribution of the M state must be larger than the M′ state. This prevents a sizable contribution from the $1/\tau'_3$ mode of the M′ state. This condition is achieved if the extinction coefficient for the M′ state is much smaller than that of the M state. However, this is probably not the case (14, 15). A second possibility is that $k_0k_{21} \gg k'_0k_{12}$. This condition is plausible but could not be tested experimentally because the phase experiment does not provide information on the light-driven steps. Using the approximations made previously for the M′ state, it is apparent that in the M state, the A_3 and A_1 contributions will have such close lifetimes as to be virtually indistinguishable. Therefore, the kinetics of the M state alone would appear biphasic. Thus, the proposed mechanism can conform to the low-salt data under a wide range of k_0 and k'_0 values.

The high-salt data show two proton transient processes of opposite amplitude. This result provides additional information over the low-salt data and allows a more quantitative testing of the mechanism. The fast proton kinetic process is not seen in the flash experiment because it does not have a sizable amplitude. As a starting point, if both τ'_1 and τ'_3 are approximately the same, then the amplitude of the fast mode of the M′ state will be larger than under low-salt conditions because it contains contributions from both modes. The ratio of the fast amplitude to the slow M′ state amplitude, R, is given by

$$R = (A'_1 + A'_3)/A'_2$$
$$= \frac{\lambda_2\tau_1(k_{12} - 1/\tau_2 + \lambda_2) - 2(1/\tau_1 - 1/\tau_2)}{\lambda_2\tau_2(-k_{12} + 1/\tau_1 - \lambda_2)}. \qquad (8)$$

To further simplify this ratio, the assumption is made that k_{12} is approximately equal to λ_1, i.e., k_1 is small. There was no a priori reason for making this assumption; rather, this condition was assumed and the resulting model tested. With the help of the simplifying relations in Eq. 7, the ratio R, was brought to the following form:

$$R = 1 - (2/\lambda_2)(1/\tau_1 - 1/\tau_2). \qquad (9)$$

Eq. 9 allows λ_2 to be estimated from a least squares fit of the experimental proton amplitude ratios shown in Table II (data above 7.3 was not used). Using the proton decay times as an estimate of τ_1 and τ_2 gives a λ_2 value of 357 s^{-1}. Using the M decay times as estimates gives a value of 255 s^{-1}. The predicted R values with these estimates are shown in Table II, where the R_1 values result from the proton decay estimates and the R_2 values result from the M decay estimates. These values agree reasonably well with the experimental ones, R^{obs}, but seem to deviate at the pH extremes. This presumably is a result of the rate constants not being totally independent of pH. The values for τ'_3 ($=1/\lambda_2$) are ~3 ms and, therefore, the initial assumption of

adding the A_3 contribution to the fast term in Eq. 8 is justified. Using Eq. 7, the λ_2 value of 357 s^{-1}, and the proton data, the average values of the following rate constants were calculated: $k_{12} = 101\ s^{-1}$, $k_2 = 317\ s^{-1}$, and $k_{21} = 40\ s^{-1}$. Using these values to calculate τ_1 and τ_2 gives values of 2.9 and 8.5 ms, respectively, which compare favorable to the observed proton lifetimes and indicate internal consistency. The value of k_{12} suggests that the A_3 term of the M intermediate should be comparable in lifetime to that of the A_2 term. Therefore, the M photocycle kinetics should show two lifetimes. Calculation of mode ratios for the photocycle kinetics is again complicated by lack of knowledge of k_0 and k_0'. The proposed mechanism explains the qualitative features of the low- and high-salt data and gives reasonable quantitative fits to the high-salt proton amplitude ratios. Thus, the three criteria described previously have been met. This shows that there is no need to evoke alternate mechanisms or proton transport stoichiometry to explain the difference in the high- and low-salt dependence.

To compare the predictions of the proposed mechanism with existing flash data, the rate equations appropriate to this different experiment are solved. In the flash experiment, an intermediate, X, is fromed rapidly and decays into the M states by two pathways. The identity of X is not important in the following discussion. The rate expressions for the proposed mechanism are:

$$-d[X]/dt = (k_0 + k_0')\,[X]$$

$$-d[M]/dt = (k_1 + k_{12})\,[M] - k_{21}[M'] - k_0[X]$$

$$-d[M']/dt = -k_{12}[M] + (k_2 + k_{21})\,[M'] - k_0'[X], \quad (10)$$

where the rate constants are defined by analogy with the phase mechanism. The boundary condition for the flash experiment is $[X] = [X]_0$ at time $t = 0$, and the concentration of all other species is zero. This boundary condition is what distinguishes the flash experiment from the phase-lifetime experiment. These equations are easily solved using the Laplace method and give the following results:

$$[M'] = \frac{[X]_0[k_0k_{21} + k_0'(\lambda_1 - k_0 - k_0')]}{(1/\tau_1 - k_0 - k_0')\,(1/\tau_2 - k_0 - k_0')}\,e^{-(k_0+k_0')t}$$

$$+ \frac{[X]_0[k_0k_{21} + k_0'(\lambda_1 - 1/\tau_1)]}{(k_0 + k_0' - 1/\tau_1)\,(1/\tau_2 - 1/\tau_1)}\,e^{-(t/\tau_1)}$$

$$+ \frac{[X]_0[k_0k_{21} + k_0'(\lambda_1 - 1/\tau_2)]}{(k_0 + k_0' - 1/\tau_2)\,(1/\tau_1 - 1/\tau_2)}\,e^{-(t/\tau_2)}. \quad (11)$$

Because of the symmetry of the mechanism, the expression for [M] is quite similar to that for [M']. It may be obtained from the above expression by interchanging k_0 and k_0' and interchanging k_{12} and k_{21}. For most conditions, these results show a monophasic rise with a biphasic decay for the M intermediates. To reproduce the observed biphasic rise would require a more complicated mechanism (using two X states that interconvert would accomplish this task). However, since this feature of the photocycle is not used in the following arguments, such complexities are avoided at this time. Note that the flash expression gives identical expressions for the relaxation times yet quite different expressions for the amplitudes. This provides a mathematical demonstration of the difference between the phase and flash techniques.

Using the above expressions, it is possible to investigate the validity of using kinetic amplitude functions to determine stoichiometry. Of special interest is a comparison of expressions for experimental parameters determined by Ort and Parsons (8) and by Grzesiek and Dencher (5). The quantum yield of proton release, Q, determined by Ort and Parsons is related to the ratio of the decay amplitudes of the M' state, $A_{M'}(\tau_1)$ and $A_{M'}(\tau_2)$ to the amount of bacteriorhodopsin photocycling, $[X]_0$. These amplitudes are obtained using Eq. 11. This is because M' is taken as the only deprotonated protein species and will be equal to the proton transient. Note that $[X]_0$ does not necessarily equal the sum of the two M decay amplitudes. Even for simple linear decay mechanisms, the amplitude of the decay process does not necessarily equal the total concentration of the initial species. The following expression is obtained for the quantum yield:

$$Q = \frac{[A_{M'}(\tau_1) + A_{M'}(\tau_2)]}{[X]_0} = \frac{-k_0k_{21} + k_0'(k_0 + k_0' - \lambda_1)}{(k_0 + k_0' - 1/\tau_1)(k_0 + k_0' - 1/\tau_2)}. \quad (12)$$

Note that in the following discussion, only the quantum yield data of Ort and Parsons are used. The H^+/M ratio determined by them is not used because it uses M concentrations determined 2 ms after the flash. This complicated function is avoided. Grzesiek and Dencher measured the ratio of the decay amplitudes of both M states, $A_{M+M'}(\tau_1) + A_{M+M'}(\tau_2)$, to the proton uptake amplitudes (M' amplitudes) (5). This ratio, R', is given by the following expression:

$$R' = 1 + \frac{k_0(k_0 + k_0 - \lambda_2) - k_0'k_{12}}{k_0'(k_0 + k_0' - \lambda_1) - k_0k_{21}}. \quad (13)$$

Experimentally, Q was shown to increase by 75% going from low to high ionic strength (8), whereas R' only decreased by 20% (5). Considering the quite different functional forms for these two parameters, this result is not necessarily inconsistent. Unfortunately, not all of the parameters are known to allow a calculation of R' and Q within the framework of the proposed model. Nevertheless, it is possible to assess if both conditions can be met with physically reasonable estimates for the parameters. From the previous analysis, the following estimates are used in the high-salt region: $\lambda_2 = 357\ s^{-1}$, $\lambda_1 = 101\ s^{-1}$, $k_{21} = 40\ s^{-1}$, $k_{12} = 101\ s^{-1}$, $1/\tau_1 = 340\ s^{-1}$, and $1/\tau_2 = 118\ s^{-1}$. The low-salt region is a little harder to estimate. The average H^+ decay time was used, giving a λ_2 estimate of 104 s^{-1}.

The average M decay times give $1/\tau_1 = 330\ s^{-1}$ and $1/\tau_2 = 67\ s^{-1}$. This results (Eq. 7) in a λ_1 value of $293\ s^{-1}$. It is more difficult to get estimates of k_{12} and k_{21} for the low-salt data. Using Eq. 7, $k_{12}k_{21}$ equals 4,040 at high salt and 8,362 at low salt. If it is assumed that all of this change is in k_{12}, then a value of $209\ s^{-1}$ can be used along with a k_{21} value of $40\ s^{-1}$. Using a search routine, k_0 and k_0' were varied and it was found that when $k_0 = 849$ and $k_0'\ 473\ s^{-1}$, the values of Q and R' changed from low salt to high salt by 1.74 and 0.79, respectively. The point of this exercise is not to propose specific values for the various parameters of the model but rather to demonstrate that there is not necessarily any inconsistency between the quantum yield results and the flash determination of $[M]/[H^+]$. The ionic strength dependence of these two parameters are consistent with the proposed model. It should be emphasized that the assumed values in this calculation do not provide stringent conditions on the model. A variety of kinetic parameters exist for which the model predicts the correct ionic strength dependence. Thus, it is seen that the proposed model is not only consistent with the phase-lifetime data presented here but also explains an apparent discrepancy in previous flash data.

DISCUSSION

Phase-lifetime spectroscopy has been used to investigate the kinetics of light-driven proton release and uptake by bacteriorhodopsin. These results are shown to have some differences to those obtained with flash techniques. This is a consequence of the different boundary conditions for the two experiments. Thus, the two techniques provide complementary but not identical information. In general, the two techniques will show processes of identical relaxation times. However, the amplitudes for these processes have a different magnitude. This is demonstrated by deriving the amplitude functions for a given mechanism for each experiments (compare Eq. 6 with Eq. 11). At low ionic strength, the two techniques give very similar results, showing the proton uptake lifetime to be intermediate between the two M decay lifetimes. At high ionic strength, the phase-lifetime results show a relaxation mode that does not have a significant amplitude in the flash experiment. This additional information is useful in evaluating photocycle mechanisms.

A single mechanism is proposed that can explain the experimental results at both high and low ionic strengths. This mechanism involves the parallel formation of two M intermediates that decay in parallel and also can interconvert. Only one of these intermediates is deprotonated (designated M'). The second intermediate (designated M) has a deprotonated Schiff base but no proton has left the protein. This mechanism explains the qualitative features of the low ionic strength data. Using one adjustable parameter (λ_2), it quantitatively explains the high ionic strength data. Very little pH dependence is seen in the range of pH 5.8–7.8, and all the high-salt data can be quantitatively fit without changing any parameters. At low ionic strength and pH 5.3, two proton transient processes are observed as in the high-salt case. At high ionic strength and pH 8.3 and 8.8, a single proton decay process is seen that is similar to the low-salt data. The behavior in these extreme ranges is not inconsistent with the mechanism, but rather shows that ionic strength and pH can have comparable effects on altering rate constants for the elementary steps.

In addition to the data presented here, the proposed mechanism can be used to explain flash results of others. Specifically, it reconciles the quantum yield data (8) with the H^+/M amplitude ratios determined from flash experiments (5). The mechanism shows that the quantum yield can vary as a result of changes of rate constants through productive and nonproductive pathways. Nevertheless, the stoichiometry of the productive pathway is fixed at one. The amplitude analysis presented here clearly demonstrates the problems associated with attempts to determine stoichiometry from kinetic data. Only in very simple mechanisms in which the individual steps are well-resolved in time will amplitude data provide an adequate measure of stoichiometry. As can be seen from Eqs. 12 and 13, quantum yield and amplitude ratios are not fixed but are dependent on specific relationships involving the rate constants. Changes in these parameters do not necessarily mean the stoichiometry or mechanism has changed.

The structure of the proposed mechanism shows a competition between a productive pathway and a nonproductive one. Any light-driven ion or electron transport process must result in a charge-separated state in the interior of the protein. Such a state would naturally have two alternate pathways; recombination of the charges (nonproductive) or a further separation of the charges to make recombination impossible (productive). The second process may be associated with a conformational change. The interconversion rates (k_{12} and k_{21}) estimated in this work puts them in the $10–10^3\ s^{-1}$ range, the time scale that protein conformational changes are expected to be on (15). Fluorescence energy transfer measurements show a significant difference in location of the retinal in the two M states, indicating that a large conformational change occurs between these two states (16). From these data alone, it is not possible to establish the vectorial nature of the proton release and uptake steps. With M' as the deprotonated intermediate, the k_0' step must be a proton release to the outside, whereas k_2 must be a proton uptake from the inside. Due to microscopic reversibility, the interconversion must result in uptake and release of protons from the same side. If the proton involved in interconversion is on the outside of the membrane, then the M state has a productive pathway available to it and the k_2 path is the only productive one available to the M' state. If the proton is on the inside, then formation of M' will always result in proton transport and formation of M will never be productive. Proton transport measurements in a vesicular

systems are required to establish the membrane orientation of the proton associated with the interconversion step.

This work was supported by a grant from the National Science Foundation (No. DMB-8315263).

Received for publication 23 June 1987 and in final form 2 October 1987.

REFERENCES

1. Ottolenghi, M. 1980. The photochemistry of rhodopsins. *Adv. Photochem.* 12:97–200.
2. Xie, A. H., J. F. Nagle, and R. H. Lozier. 1987. Flash spectroscopy of purple membrane. *Biophys. J.* 51:627–635.
3. Sherman, W. V., R. R. Eicke, S. R. Stafford, and F. M. Wasacz. 1979. Branching in the bacteriorhodopsin photocycle. *Photochem. Photobiol.* 30:727–729.
4. Govindjee, R., T. G. Ebrey, and A. R. Crofts. 1980. The quantum efficiency of proton pumping by the purple membrane of *Halobacterium halobium*. *Biophys. J.* 30:231–242.
5. Grzesiek, S., and N. A. Dencher. 1986. Time-course and stoichiometry of light-induced proton release and uptake during the photocycle of bacteriorhodopsin. *FEBS (Fed. Eur. Biochem. Soc.) Lett.* 208:337–342.
6. Lozier, R. H., W. Niederberger, R. A. Bogomolni, S. B. Hwang, and W. Stoeckenius. 1976. Kinetics and stoichiometry of light-induced proton release from purple membrane fragments, Halobacterium halobium cell envelopes, and phospholipid vesicles containing oriented purple membrane. *Biochem. Biophys. Acta.* 440:545–546.
7. Drachev, L. A., A. D. Kaulen, and V. P. Skulachev. 1984. Correlation of photochemical cycle, H^+ release and uptake, and electric events in bacteriorhodopsin. *FEBS (Fed. Eur. Biochem. Soc.) Lett.* 178:331–335.
8. Ort, D. R., and W. W. Parsons. 1979. The quantum yield of flash-induced proton release by bacteriorhodopsin-containing membrane fragments. *Biophys. J.* 25:341–354.
9. Dewey, T. G. 1987. Phase-lifetime spectroscopy of photocycle processes. *Biophys. J.* 51:809–815.
10. Lanyi, J. K., and R. E. MacDonald. 1979. Light-induced transport in Halobacterium halobium. *Methods Enzymol.* 56:398–407.
11. Becher, B., and J. Y. Cassim. 1975. Improved isolation procedures for the purple membrane of Halobacterium halobium. *Prep. Biochem.* 5:161–178.
12. Dewey, T. G., and G. G. Hammes. 1981. Methods for studying kinetics of light-induced transport across membranes. *Proc. Natl. Acad. Sci. USA.* 78:7422–7425.
13. Hasselbacher, C. A., D. K. Preuss, and T. G. Dewey, 1986. Location of the retinal of bacteriorhodopsin's M_{412} intermediates by phase modulation of resonance energy transfer. *Biochemistry.* 25:668–676.
14. Rosenbach, V., R. Goldberg, C. Gilon, and M. Ottolenghi. 1982. On the role of tyrosine in the photocycle of bacteriorhodopsin. *Photochem. Photobiol.* 36:197–201.
15. Fersht, A. 1985. Enzyme Structure and Mechanism. W. H. Freeman and Co., New York. 152–153.
16. Hasselbacher, C. A., and T. G. Dewey. 1986. Changes in retinal position during the bacteriorhodopsin photocycle: a resonance energy transfer study. *Biochemistry.* 25:6236–6243.